

Nucleation of superfluid-light domains in a quenched dynamics

Joaquín Figueroa^{1,2}, José Rogan^{1,2}, Juan Alejandro Valdivia^{1,2}, Miguel Kiwi^{1,2}, Guillermo Romero³, and Felipe Torres^{1,2,†}

¹Departamento de Física, Facultad de Ciencias, Universidad de Chile, Casilla 653, Santiago, Chile 7800024

²Center for the Development of Nanoscience and Nanotechnology 9170124, Estación Central, Santiago, Chile

³Departamento de Física, Universidad de Santiago de Chile (USACH), Avenida Ecuador 3493, 9170124, Santiago, Chile

†felestorres@gmail.com

ABSTRACT

Strong correlation effects emerge from light-matter interactions in coupled resonator arrays, such as the Mott-insulator to superfluid phase transition of atom-photon excitations. We demonstrate that the quenched dynamics of a finite-sized complex array of coupled resonators induces a first-order like phase transition. The latter is accompanied by domain nucleation that can be used to manipulate the photonic transport properties of the simulated superfluid phase; this in turn leads to an empirical scaling law. This universal behavior emerges from the light-matter interaction and the topology of the array. The validity of our results over a wide range of complex architectures might lead to a promising device for use in scaled quantum simulations.

Introduction

The absence of energy dissipation in the flow dynamics of a quantum fluid is one of the most fascinating effects of strongly correlated condensates^{1–6}. Quantum phase transitions, from Mott insulator to superfluid, have been observed in a wide range of physical platforms such as ultracold atoms in optical lattices⁷, trapped gases of interacting fermionic atom pairs⁸, and exciton-polariton condensates^{9–11}. Furthermore, the remarkable progress in controlling light-matter interactions in the microwave regime of circuit quantum electrodynamics (QED) has provided a suitable scenario for studying strongly correlated effects with light^{12–14}. In this case, coupled resonator arrays (CRAs) each doped with a two-level system (TLS) allow for the formation of dressed quantum states (polaritonic states) and effective photon-photon interactions. The underlying physics is well described by the Jaynes-Cummings-Hubbard (JCH) model^{15–17}. In this case, if the frequencies of the single resonator mode and the TLS are close to resonance, the effective photonic repulsion prevents the presence of more than one polaritonic excitation in the resonator, due to the photon-blockade effect^{18–20}. Detuning the atomic and photonic frequencies diminishes this effect and leads the system to a photonic superfluid¹⁶. Unlike Bose-Einstein condensation in optical lattices, polariton condensation includes two kind of excitations, atomic and photonic, and the transition from Mott-insulator to superfluid is accompanied by a transition of the excitations from polaritonic to photonic¹⁶.

Here we show how a first-order like phase transition of the simulated superfluid phase of polaritons in CRAs can be induced by a quench dynamics as described by the JCH model. We compare full numerical simulations of several arrangements of CRAs with mean-field theory of photonic fluctuations dynamics. In this case, the simulated Mott-superfluid transition relies on the topological properties of the array, since the on-site photon blockade strongly depends on the connectivity of each node, even for small resonator-resonator hopping strength. When the system is prepared in the Mott state with a filling factor of one net excitation per site, and a sudden quench of the detuning between the single resonator mode and the TLS is applied, we find a first-order like phase transition which can be described by two bosonic excitations of the lower and upper polariton band. We find that a nucleated superfluid photon state emerges in a localized way, which depends on the topology of the array. This avalanche-like behavior near the simulated phase transition leads to a universal scaling law between critical parameters of the superfluid phase and the average connectivity of the array.

The model

The physical scenario that we consider are CRAs in complex arrangements such as the one in Fig. 1(a). Here, each node of the array consists of a QED resonator doped with a TLS to be a real or artificial atom, and the whole

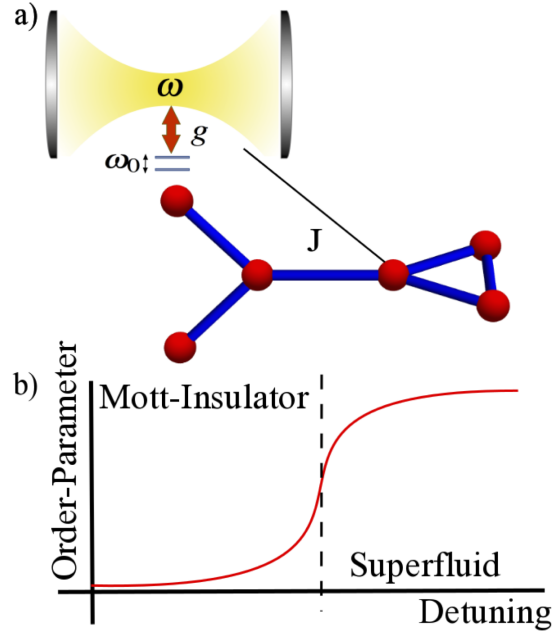


Figure 1. (color online) a) Schematic representation of the Jaynes-Cummings-Hubbard lattice in a complex array where each node consists of a single resonator strongly coupled to a two-level system. b) Phase transition from Mott-insulator to superfluid in light-matter CRAs systems as a function of the detuning parameter.

system is described by the Jaynes-Cummings-Hubbard model^{15–17}, whose Hamiltonian reads

$$H_{JCH} = \sum_{i=1}^L H_i^{JC} - J \sum_{\langle i,j \rangle} A_{ij} a_i^\dagger a_j + \text{h.c.} - \sum_{i=1}^L \mu_i n_i, \quad (1)$$

where L is the number of lattice sites, a_i (a_i^\dagger) is the annihilation (creation) bosonic operator, J is the photon-photon hopping amplitude, A_{ij} is the adjacency matrix which takes values $A_{ij} = 1$ if two sites of the lattice are connected and $A_{ij} = 0$ otherwise. μ_i stands for the chemical potential at site i and $n_i = a_i^\dagger a_i + \sigma_i^+ \sigma_i^-$ represents the number of polaritonic excitations at site i . Also, $H_i^{JC} = \omega a_i^\dagger a_i + \omega_0 \sigma_i^+ \sigma_i^- + g(\sigma_i^+ a_i + \sigma_i^- a_i^\dagger)$ is the Jaynes-Cummings (JC) Hamiltonian describing light-matter interaction²¹. Here, σ_i^+ (σ_i^-) is the raising (lowering) operator acting on the TLS Hilbert space, and ω , ω_0 , and g are the resonator frequency, TLS frequency, and light-matter coupling strength, respectively. Notice that the total number of elementary excitations (polaritons) in this system $N = \sum_i^M (a_i^\dagger a_i + \sigma_i^+ \sigma_i^-)$ is the conserved quantity $[N, H_{JCH}] = 0$ ^{22,23}.

The quantum dynamics of this model has been studied for linear lattices^{15,16}, and its equilibrium properties at zero temperature have been studied by means of density matrix renormalization group², and by means of mean field (MF) theory, for two-dimensional lattices^{17,25,26} and complex networks²⁷. The latter studies have provided evidence of a quantum phase transition from Mott-insulating phases to a superfluid polaritonic phase. Beyond the MF approach there have been important contributions from the numerical and analytical viewpoint for extracting the phase boundaries^{28–32}, the study of critical behavior^{30–32}, and the excitation spectrum^{29,31,32}. For a general overview on many-body physics with light relevant literature is available^{33–35}.

Mott-insulator to superfluid phase transition

Here we briefly summarize the Mott-insulator to superfluid phase transition in the JCH model¹⁶. Our main results are focused on the quantum dynamics of the JCH model (1) in complex networks, where we focus on the canonical

ensemble with a fixed total number of polaritons^{13,14}. In this case, the JCH Hamiltonian reads

$$H_{\text{JCH}} = \sum_{i=1}^L H_i^{\text{JC}} - J \sum_{\langle i,j \rangle} A_{ij} a_i^\dagger a_j + \text{h.c.} \quad (2)$$

In the atomic limit, where the photon-hopping can be neglected ($J \ll g$), the JC Hamiltonian at site i (H_i^{JC}) can be diagonalized in the polaritonic basis that mixes atomic and photonic excitations $|n, \pm\rangle_i = \gamma_{n\pm} |\downarrow, n\rangle_i + \rho_{n\pm} |\uparrow, n-1\rangle_i$ with energies $\epsilon_n^\pm = n\omega + \Delta/2 \pm \chi(n)$, where $\chi(n) = \sqrt{\Delta^2/4 + g^2 n}$, $\rho_{n+} = \cos(\theta_n/2)$, $\gamma_{n+} = \sin(\theta_n/2)$, $\rho_{n-} = -\gamma_{n+}$, $\gamma_{n-} = \rho_{n+}$, $\tan \theta_n = 2g\sqrt{n}/\Delta$, and the detuning parameter $\Delta = \omega_0 - \omega$.

Now, one can introduce the polaritonic creation operators at site i defined as $P_i^{\dagger(n,\alpha)} = |n, \alpha\rangle_i \langle 0, -|$, where $\alpha = \pm$ and we identify $|0, -\rangle \equiv |\downarrow, 0\rangle$ and $|0, +\rangle \equiv |\emptyset\rangle$ being a ket with all entries equal to zero, that is, it represents an unphysical state. These identifications imply $\gamma_{0-} = 1$ and $\gamma_{0+} = \rho_{0\pm} = 0$. Using this polaritonic mapping the Hamiltonian (2) can be rewritten as^{16,26}

$$H = \sum_{i=1}^L \sum_{n=1}^{\infty} \sum_{\alpha=\pm} \epsilon_n^\alpha P_i^{\dagger(n,\alpha)} P_i^{(n,\alpha)} - J \sum_{\langle i,j \rangle} A_{ij} \left[\sum_{n,m=1}^{\infty} \sum_{\alpha,\alpha',\beta,\beta'} t_{\alpha,\alpha'}^n t_{\beta,\beta'}^m P_i^{\dagger(n-1,\alpha)} P_i^{(n,\alpha')} P_j^{\dagger(m,\beta)} P_j^{(m-1,\beta')} + \text{h.c.} \right], \quad (3)$$

where the matrix elements $t_{\alpha,\alpha'}^n$ are given by $t_{\pm+}^n = \sqrt{n}\gamma_{n\pm}\gamma_{(n-1)+} + \sqrt{n-1}\rho_{n\pm}\gamma_{(n-1)-}$ and $t_{\pm-}^n = \sqrt{n}\gamma_{n\pm}\rho_{(n-1)+} + \sqrt{n-1}\rho_{n\pm}\rho_{(n-1)-}$. The first term in Eq. (3) stands for the local polaritonic energy with an anharmonic spectrum and gives rise to an effective on-site polaritonic repulsion. The last term in Eq. (3) represents the polariton hopping between nearest neighbors and long range sites, and it may also allow for the interchange of polaritonic excitations.

If the physical parameters of the Hamiltonian (3) are in the regime $Jn \ll g\sqrt{n} \ll \omega$, and for an integer filling factor, where the total number of excitations N over the lattice is an integer multiple of the number of unit cells L , the lowest energy state is the product $\bigotimes_{i=1}^L |1, -\rangle_i$ which corresponds to a Mott-insulating phase, and its associated energy is $E = N\epsilon_1^-$. In the thermodynamics limit, the interplay between the on-site polariton repulsion and the polariton hopping leads to a phase transition from a Mott insulator to a superfluid phase. The latter may be reached by diminishing the on-site repulsion by means of detuning the atomic and photonic frequencies. At equilibrium, this phase transition may be quantified by means of bipartite fluctuations^{1,2}. In a simulated Mott-insulator transition, where an adiabatic dynamics drives the passage, it has been shown that a suitable order parameter corresponds to the variance of the number of excitations per site. Fig. 1(b) shows the archetypal behavior of the order parameter as a function of the detuning Δ in the adiabatic dynamic regime, and for an integer filling factor of one net excitation per site¹⁶.

Quenched dynamics and Topology in finite-size complex lattices.

Our aim is to describe how complex arrangements of CRAs, such as the one appearing in Fig. 1(a), affect the simulated phase transition from Mott insulator to superfluid as the detuning parameter Δ is suddenly quenched. In particular, we are interested in how one can manipulate photonic transport properties of the emerging superfluid phase depending on the specific topology of the CRAs. As order parameter we choose the time-averaged standard deviation of the polariton number $\frac{1}{T} \int_0^T dt \sum_{i=1}^L (\langle n_i^2 \rangle - \langle n_i \rangle^2)$ with $T = J^{-1}$, and we assume the whole system initially prepared in the Mott-insulating state $|\psi_0\rangle = \bigotimes_{i=1}^L |1, -\rangle_i$, with $\Delta = 0$ at each lattice site. In the supplementary material we present another equivalent measures of the order parameter based on the bipartite fluctuation proposed by S. Rachel *et al.*¹, and D. Rossini *et al.*². Of course, due to computational restrictions, we consider relatively small arrangements of CRAs, but with varying degrees of complexity, suggesting that the topology of the network could be used in a nontrivial way to manipulate the emerging of the superfluid phase as these system becomes larger and approach the thermodynamical limit.

The initialization process may be achieved by the scheme proposed by Angelakis *et al.*¹⁶. For instance, in circuit QED^{13,14} one might cool down the whole system reaching temperatures around $T_0 \sim 15\text{mK}$. In this case, the system will be prepared in its global ground state $|G\rangle = \bigotimes_{i=1}^L |0, -\rangle_i$. Then, one can apply individual magnetic fields on the TLSs, each implemented via a transmon qubit³⁷, such that the resonance condition $\Delta = 0$ is achieved. This way one can address individually each cavity with an external AC microwave current or voltage tuned to the transition $|\downarrow, 0\rangle_i \rightarrow |1, -\rangle_i$, with a driving frequency $\omega_D = \omega - g$, such that the system will be prepared in the desired initial

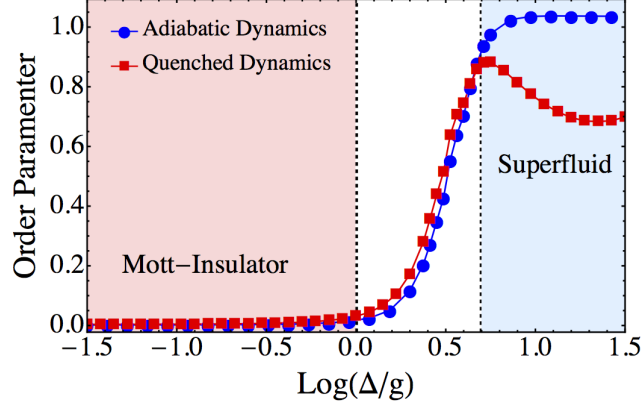


Figure 2. (color online) Quantum phase transition of a dimer array. Detuning dependence of the order parameter with two TLS coupled through photon hopping, adiabatic dynamics (blue circles) and quench dynamics (red squares). Continuous lines have been added as guide to the eye.

state $|\psi_0\rangle$. The sudden quench of the detuning can be achieved by applying magnetic fields to the transmon qubits in order to reach the desired superfluid phase. It is noteworthy that when the initial state is a linear superposition of upper and lower polariton states ($\Delta \neq 0$) the quantum dynamics will be dominated by these two polaritonic bands. Also, we carry out full numerical calculations for the parameters $g = 10^{-2}\omega$ and $J = 10^{-2}g$, and we consider up to 6 Fock states per bosonic mode. These parameter values allow us to prevent the interchange of polaritonic excitations between different sites.

In order to gain insight into the quench dynamics of the topological CRAs let us consider a dimer array. As shown in Fig. 2, the simulated Mott-insulator to Superfluid phase transition strongly depends on the type of dynamics. Adiabatic dynamics resembles a second order phase transition which leads to a continuous change of the state of the system. On the other hand, the quench dynamics takes place accompanied by a discontinuous change of the state, analogous to the Metal-Insulator transition of oxides³⁸. Hence, as we expected, the adiabatic dynamics is not qualitatively affected by the distribution of nearest neighbors. However, the topological properties of the array dominate a first-order like phase transition driving the quench dynamics (see Fig. 2). As the degree of inter-connectivity between the resonators grows the distance between them rapidly diminishes, and thus local correlations become more important due to quantum interference effects. If scaled up to the size of the system, due to the increase in the degrees of freedom, the numerical simulation time grows exponentially. In the next section we obtain an empirical scaling law to address this issue. Indeed, we demonstrate that the photon propagation in the simulated superfluid phase strongly depends of the connectivity per site $k_i = \sum_j A_{ij}$. Let us consider a set of arrays with a fixed number of TLS. As shown in Fig. 3(a) in the quench dynamics case the averaged standard deviation depends linearly on the connectivity, which means that depending on the connectivity the local superfluid states are reached with different detuning scales. We consider a set of CRAs with four and five interconnecting resonators as shown in Fig. 3(b). In contrast to these results, the adiabatic dynamics does not exhibit a monotone or linearly growing behavior, which leads to a sharper phase transition, as illustrated in Fig. 2.

Mean-field theory of the Superfluid Phase

In the thermodynamics limit, the emergent superfluid phase behaves as a quantum liquid¹⁷. Superfluidity is achieved by means of a transition of the excitations from polaritonic to photonic. In order to describe the simulated superfluid phase in our system, we introduce the photonic order parameter¹⁷ $\psi = \langle a_i \rangle$. Using the decoupling approximation $a_i^\dagger a_j \approx \langle a_i^\dagger \rangle a_j + a_i^\dagger \langle a_j \rangle - \langle a_i^\dagger \rangle \langle a_j \rangle$, the resulting mean-field JCH Hamiltonian can be written as

$$H_{JCH} = \sum_i H_i^{JC} - J \sum_i k_i (\psi a_i^\dagger + \psi^* a_i). \quad (4)$$

Therefore, the simulated Mott-insulator phase can be characterized by the on site repulsion, which suppresses the fluctuations of the number of per site excitations $|\psi| = 0$. On the contrary, the superfluid phase is dominated by the hopping and the quantum fluctuations $|\psi| \neq 0$. Now we focus on the light-matter coupling induced by the hopping of

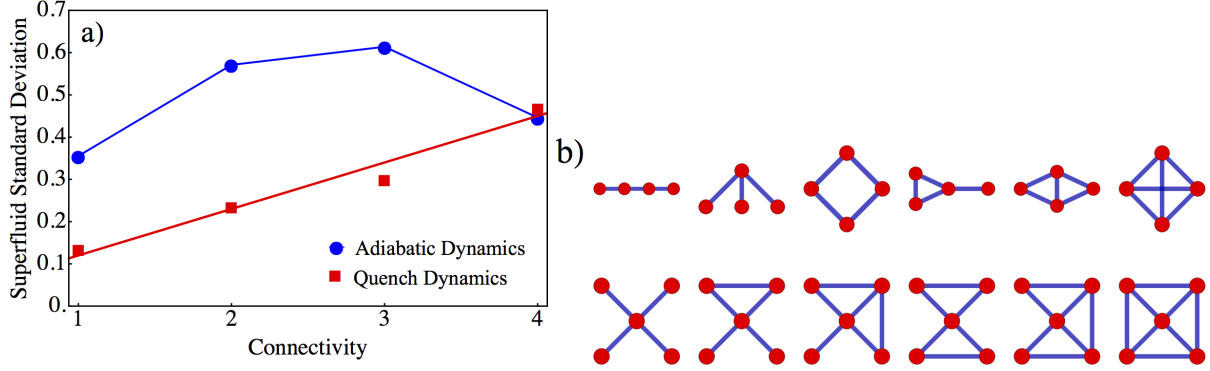


Figure 3. (color online) a) Standard deviation of the superfluid phase as a function of the connectivity. Adiabatic dynamics (blue circles) and quench dynamics (red squares). A set of CRAs with four and five interconnecting resonators, as shown in b) are considered. Continuous lines have been added as a guide to the eye.

photons through cavities. Introducing the identity $\sigma^+\sigma^- + \sigma^-\sigma^+ = \mathbb{1}$, we obtain an effective light-matter coupling, since it retains the mixed products of photonic and two level operators,

$$h_i^{LM} = \tilde{g}_i a_i^\dagger \sigma_i^- + \tilde{g}_i^\dagger a_i \sigma_i^+ + \text{h.c.} \quad (5)$$

Here $\tilde{g}_i = \mathbb{1}g/2 - Jk_i\psi^*\sigma_i^-$ is the effective light-matter coupling per site, which therefore turns out to be an operator. In the simulated superfluid phase the atomic transitions are expected to be suppressed against the photonic dressed states. Moreover, the total excitation number does not change, hence when the photonic excitations increase the atomic excitations decrease. Note that when $\tilde{g}_i = \mathbb{1}g$, i.e. when there are no hopping or topological effects,

$$\langle \sigma_i^+ \rangle = \frac{g}{Jk_i\psi}, \quad (6)$$

which indicates that the total number of excitations is conserved and also demonstrates that the increase of the photonic states leads to a reduction of the atomic excitations, due to the conservation of the number excitations. Fig. 4 shows the effect of the quench dynamics on the simulated phase transition of the JCH model for different arrays. In this case the nucleation of superfluid states emerges due to the variation of the order parameter, according to Eq. (6). In the Mott-Insulator state $\langle \sigma_i^+ \rangle > 0 \forall i$, when the detuning is increased $\langle \sigma_i^+ \rangle$ decreases by a factor $1/(k_i\psi)$, until the superfluid phase is reached.

We have shown that the mean field approach strongly supports the scaling law of the order parameter shown in Fig. 3(a); namely, as the connectivity of CRAs is increased locally, the light superfluid phase is achieved for a smaller detuning strength.

Conclusion

We show that quench dynamics induce a first-order like phase transition in coupled resonator arrays doped with a two-level system. The nucleation of simulated superfluid states has been demonstrated by numerical simulation and by a mean field theoretical approach. In the quench dynamics the abrupt change of the order parameter, instead of sharper crossover driven by adiabatic dynamics, is explained by the non uniform transition from Mott-Insulator to superfluid, which locally depends of the connectivity. Since the quench dynamics exhibits the same behavior independent of the choice of the order parameter, the standard deviation of the polariton number or the bipartite fluctuation, our results reveal the universality of the simulated first order phase transition (also see Supplementary Material). As the number of TLS is increased the averaged standard deviation of the superfluid phase depends linearly on the connectivity. At an increased scale, for large networks of doped optical/microwave resonators, our system may enter the field of quantum simulators. In particular, as far as we understand, there is no known microscopic mechanism for predicting nucleation in first-order phase transitions. In this context, our results provide an exact geometrical description for the appearance of domain nucleation due to the number of connections. Thus, our results may be used to predict, and manipulate, the nucleation of a superfluid phase of light in complex-random networks.

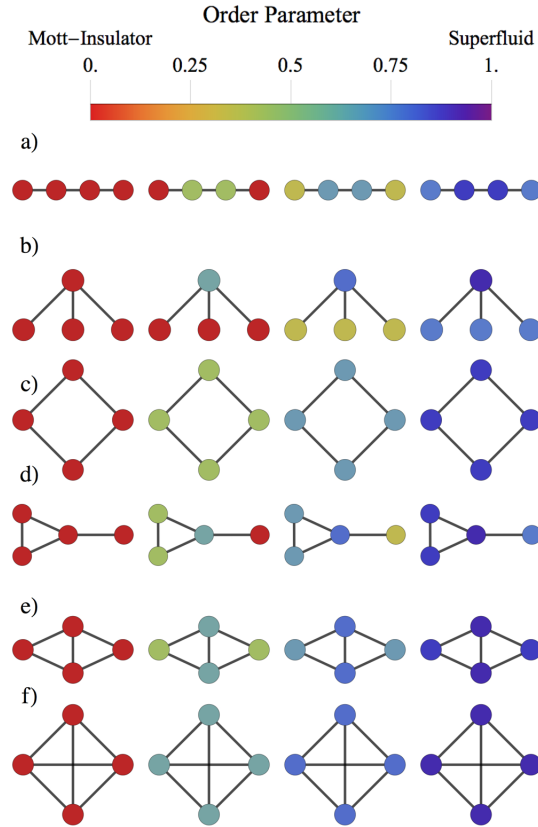


Figure 4. (color-online) Numerical simulation of the quench dynamics. The full set of four node arrays, with (a-b) three; (c-d) four; (e) five; and (f) six connections. Connectivity per site a) (1,2,2,1), b) (1,1,1,3), c) (2,2,2,2), d) (1,3,2,2), e) (2,3,3,2), and f) (3,3,3,3). As the connectivity is increased locally the superfluid phase is achieved with a lower detuning strength. For each array and from left to right we have considered parameters $\log(\Delta/g) = (0.5, 0.7, 0.75, 0.8)$, and $g = 10^{-2}\omega$, $J = 10^{-3}\omega$, where ω is the resonator frequency.

References

1. P. Kapitza, *Nature* **141**, 74 (1938).
2. A. J. Leggett, *Quantum Liquids* (Oxford University Press, 2006).
3. M. H. Anderson, J. R. Ensher, M. Matthews, C. E. Wieman, and E. A. Cornell, *Science* **269**, 198 (1995).
4. R. Onofrio, C. Raman, J. M. Vogels, J. R. Abo-Shaeer, A. P. Chikkatur, and W. Ketterle, *Phys. Rev. Lett.* **85**, 2228 (2000), URL <https://link.aps.org/doi/10.1103/PhysRevLett.85.2228>.
5. M. W. Zwierlein, C. A. Stan, C. H. Schunck, S. M. F. Raupach, S. Gupta, Z. Hadzibabic, and W. Ketterle, *Phys. Rev. Lett.* **91**, 250401 (2003), URL <https://link.aps.org/doi/10.1103/PhysRevLett.91.250401>.
6. M. Schiró, M. Bordyuh, B. Öztop, and H. E. Türeci, *Phys. Rev. Lett.* **109**, 053601 (2012), URL <https://link.aps.org/doi/10.1103/PhysRevLett.109.053601>.
7. M. Greiner, O. Mandel, T. Esslinger, T. W. Hansch, and I. Bloch, *Nature* **415**, 39 (2002), URL <http://dx.doi.org/10.1038/415039a>.
8. C. A. Regal, M. Greiner, and D. S. Jin, *Phys. Rev. Lett.* **92**, 040403 (2004), URL <https://link.aps.org/doi/10.1103/PhysRevLett.92.040403>.
9. G. Lerario, A. Fieramosca, F. Barachati, D. Ballardini, K. S. Daskalakis, L. Dominici, M. De Giorgi, S. A. Maier, G. Gigli, S. Kena-Cohen, et al., *Nat Phys* **13**, 837 (2017), URL <http://dx.doi.org/10.1038/nphys4147>.
10. E. Wertz, L. Ferrier, D. D. Solnyshkov, R. Johné, D. Sanvitto, A. Lemaître, I. Sagnes, R. Grousseau, A. V. Kavokin, P. Senellart, et al., *Nat Phys* **6**, 860 (2010).
11. T. Byrnes, N. Y. Kim, and Y. Yamamoto, *Nat Phys* **10**, 803 (2014).

12. A. A. Houck, H. E. Türeci, and J. Koch, *Nat Phys* **8**, 292 (2012).
13. J. Raftery, D. Sadri, S. Schmidt, H. E. Türeci, and A. A. Houck, *Phys. Rev. X* **4**, 031043 (2014), URL <https://link.aps.org/doi/10.1103/PhysRevX.4.031043>.
14. M. Fitzpatrick, N. M. Sundaresan, A. C. Y. Li, J. Koch, and A. A. Houck, *Phys. Rev. X* **7**, 011016 (2017), URL <https://link.aps.org/doi/10.1103/PhysRevX.7.011016>.
15. M. J. Hartmann, F. G. S. L. Brandao, and M. B. Plenio, *Nat Phys* **2**, 849 (2006).
16. D. G. Angelakis, M. F. Santos, and S. Bose, *Phys. Rev. A* **76**, 031805 (2007).
17. A. D. Greentree, C. Tahan, J. H. Cole, and L. C. L. Hollenberg, *Nat Phys* **2**, 856 (2006), URL <http://dx.doi.org/10.1038/nphys466>.
18. K. M. Birnbaum, A. Boca, R. Miller, A. D. Boozer, T. E. Northup, and H. J. Kimble, *Nature* **436**, 87 (2005), URL <http://dx.doi.org/10.1038/nature03804>.
19. A. Imamoglu, H. Schmidt, G. Woods, and M. Deutsch, *Phys. Rev. Lett.* **79**, 1467 (1997), URL <https://link.aps.org/doi/10.1103/PhysRevLett.79.1467>.
20. A. D. Greentree, J. A. Vaccaro, S. R. de Echaniz, A. V. Durrant, and J. P. Marangos, *Journal of Optics B: Quantum and Semiclassical Optics* **2**, 252 (2000), URL <http://stacks.iop.org/1464-4266/2/i=3/a=306>.
21. E. T. Jaynes and F. W. Cummings, *Proceedings of the IEEE* **51**, 89 (1963), ISSN 0018-9219.
22. M. Hartmann, F. Brandão, and M. Plenio, *Laser & Photonics Reviews* **2**, 527 (2008), ISSN 1863-8899.
23. M. J. Hartmann and M. B. Plenio, *Physical Review Letters* **99**, 103601 (2007).
24. D. Rossini, R. Fazio, and G. Santoro, *EPL* **83**, 47011 (2008), URL <http://iopscience.iop.org/article/10.1209/0295-5075/83/47011?pageTitle=IOPscience>.
25. N. Na, S. Utsunomiya, L. Tian, and Y. Yamamoto, *Phys. Rev. A* **77**, 031803 (2008).
26. J. Koch and K. Le Hur, *Phys. Rev. A* **80**, 023811 (2009), URL <https://link.aps.org/doi/10.1103/PhysRevA.80.023811>.
27. A. Halu, S. Garnerone, A. Vezzani, and G. Bianconi, *Phys. Rev. E* **87**, 022104 (2013).
28. D. Rossini and R. Fazio, *Phys. Rev. Lett.* **99**, 186401 (2007).
29. M. Aichhorn, M. Hohenadler, C. Tahan, and P. B. Littlewood, *Phys. Rev. Lett.* **100**, 216401 (2008).
30. J. Zhao, A. W. Sandvik, and K. Ueda, Preprint arXiv:0806.3603 (2008).
31. P. Pippian, H. G. Evertz, and M. Hohenadler, *Phys. Rev. A* **80**, 033612 (2009).
32. S. Schmidt and G. Blatter, *Phys. Rev. Lett.* **103**, 086403 (2009).
33. M. J. Hartmann, *J. Opt.* **18**, 104005 (2016), URL <http://iopscience.iop.org/article/10.1088/2040-8978/18/10/104005/meta>.
34. C. Noh and D. G. Angelakis, *Rep. Prog. Phys.* **80**, 016401 (2016), URL <http://iopscience.iop.org/article/10.1088/0034-4885/80/1/016401>.
35. D. G. Angelakis, ed., *Quantum Simulations with Photons and Polaritons*, Quantum Science and Technology (Springer, 2017).
36. S. Rachel, N. Laflorencie, H. Francis Song, and K. Le Hur, *Phys. Rev. Lett.* **108**, 116401 (2012), URL <https://link.aps.org/doi/10.1103/PhysRevLett.108.116401>.
37. J. Koch, T. M. Yu, J. Gambetta, A. A. Houck, D. I. Schuster, J. Majer, A. Blais, M. H. Devoret, S. M. Girvin, and R. J. Schoelkopf, *Phys. Rev. A* **76**, 042319 (2007), URL <https://link.aps.org/doi/10.1103/PhysRevA.76.042319>.
38. Marcelo J. Rozenberg, *Phys. Rev. B* **55**, R4855 (1997), URL <https://journals.aps.org/prb/abstract/10.1103/PhysRevB.55.R4855>.

Acknowledgements

This work was supported by the Fondo Nacional de Investigaciones Científicas y Tecnológicas (FONDECYT, Chile) under grants No. 1150806 (FT), No. 1160639 (MK, JR), 1150718 (JAV), 1150653 (GR), Grant-FA9550-16-1-0122 (FT, MK), CEDENNA through the “Financiamiento Basal para Centros Científicos y Tecnológicos de Excelencia-FB0807” and AWARD NO. FA9550-18-1-0438 (FT, JR, MK and JAV).

Supplementary Material: Nucleation of superfluid-light domains in a quenched dynamics

Integration time

In the definition of the order parameter, namely, using the variance of the polariton number or the bipartite fluctuations of the polariton number, we integrate fluctuations up to a time $T = 1/J$, which is a characteristic time scale where the hopping strength dominates the dynamics, thus producing a delocalized wave function over different lattice points.

However, for longer simulation times, there are no significant differences in the behavior of the studied order parameter. We have carried out numerical simulations for the dimer, and for a linear array of three coupled resonators; the results are shown in Fig. (5). We see that the order parameter for different integration times exhibits the same qualitative behavior. Also, for times $t < 1/J$, not shown here, the studied order parameter almost vanishes and we do not see the crossover of the Mott-insulator to superfluid.

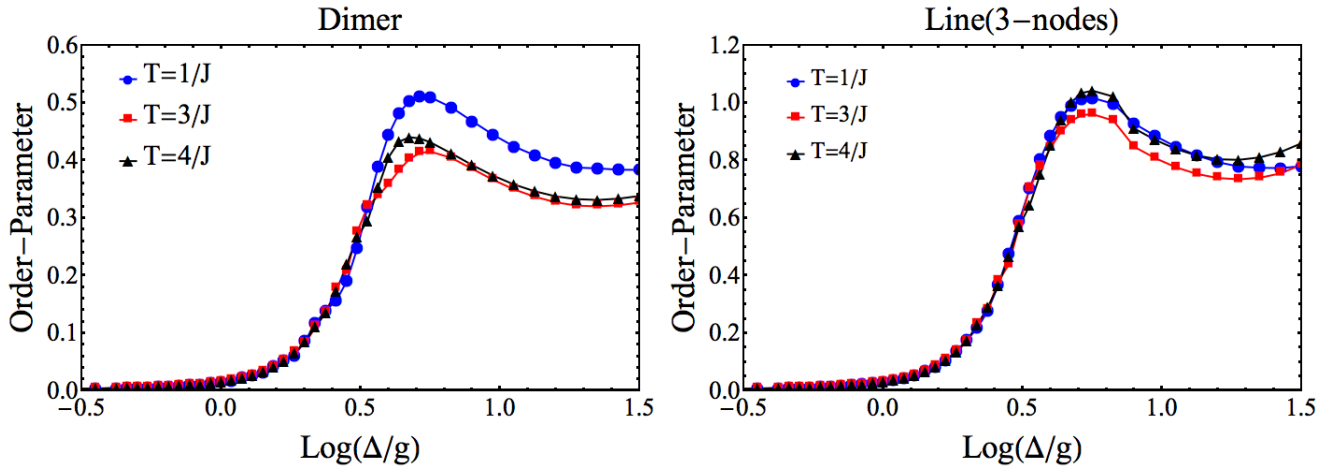


Figure 5. (color-online) Order parameter as a function of the detuning for different integration times ($T = 1/J, 3/J$, and $4/J$). As the size of the array is increased there is no significant change in the standard deviation of the superfluid phase.

Describing Simulated First Order Phase Transition using Bipartite Fluctuations

The polariton number is conserved in our system since it does not exchange particles with the outside. Hence for both detuning $\Delta = 0$ and $\Delta \gg g$, where g stands for the light-matter coupling strength, the corresponding (simulated) Mott and superfluid states are described by Fock states. This way, if one considers the standard order parameter studied in mean-field approximation, that is, the average value of the annihilation operator per site, it will always be zero and will not capture any crossover from Mott insulator to superfluid. This is why we choose to study the simulated phase transition using the onsite variance of the polariton number. However, we demonstrate that the first-order like-behavior is universal, in the sense that it does not depend on the choice of the order parameter. Indeed, if we use the bipartite fluctuations of subsystems we find that this approach also provides a correct description of the Mott to superfluid phase transition. Certainly, the dispersion of the polariton number on a given partition M -th can be assessed by the variance of this subsystem, which can be obtained from the two-point correlation function $C_{i,j} = \langle n_i n_j \rangle - \langle n_i \rangle \langle n_j \rangle$, using the parameter $\sum_{i,j \in M} C_{ij}$, where n_i denotes the polariton occupation number at the i -th site,^{1,2}

We have performed numerical calculations for bipartite fluctuations in our finite arrays. Thus we can demonstrate that a simulated first order phase transition appears regardless of the choice of the order parameter; see left-panel of Fig. (6). As shown in the right-panel of the Fig. (6), using the bipartite fluctuations approach, the averaged standard deviation also displays a linear dependence on the connectivity of the partition.

Where the connectivity of the partition has been defined as the ratio between the external connectivity (total number of links between one node in the partition and the external nodes) of each node and the total number of nodes. The connectivity of the partition are summarized in Table 1. These results demonstrated the linear

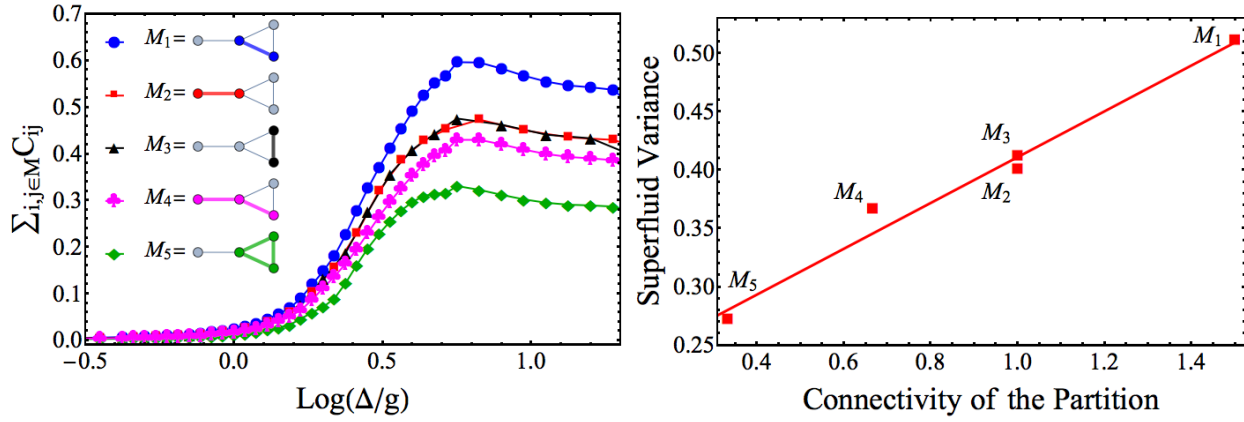


Figure 6. (color-online) (left) Bipartite fluctuations of polariton occupation number belonging to the M -th partition as a function of detuning. (right) Standard deviation of the superfluid phase as a function of the connectivity of the M -th partition.

dependence of the order between the connectivity and the order parameter, in both case, when the order parameter is identified as the standard deviation or as the variance of the bipartite fluctuations.

Partition	External connectivity	Number of Nodes	Connectivity of the partition
M_1	2+1	2	3/2
M_2	2	2	2/2
M_3	2	2	2/2
M_4	2	3	2/3
M_5	1	3	1/3

Table 1. Summary of the connectivity of each partition corresponding to the array of the inset of Fig. (6-left). The variance of the superfluid phase depends linearly on the connectivity of the partition, as shown in Fig. (6-right)

References

1. S. Rachel, N. Laflorencie, H. Francis Song, and K. Le Hur, *Phys. Rev. Lett.* **108**, 116401 (2012), URL <https://link.aps.org/doi/10.1103/PhysRevLett.108.116401>.
2. D. Rossini, R. Fazio, and G. Santoro, *EPL* **83**, 47011 (2008), URL <http://iopscience.iop.org/article/10.1209/0295-5075/83/47011?pageTitle=IOPscience>.